Design of bounded and partially bounded tracking controllers for DC motors

Luis Monay Arredondo
PhD student
TecNM-Instituto Tecnológico de Tijuana
Tijuana, BC, Mexico
ORCID 0000-0001-6034-7020

Claudia Loreto-Medina
TecNM - Instituto Tecnológico de Tijuana
Tijuana, BC, Mexico
ORCID 0000-0003-3264-2668

Eddie Clemente
TecNM - CENIDET
Cuernavaca, Morelos, Mexico
ORCID 0000-0003-3195-9540

Marlen Meza-Sánchez
TecNM-Instituto Tecnológico de Tijuana
Tijuana, BC, Mexico
ORCID 0000-0002-1853-5607

Leonardo Herrera
Naval Postgraduate School
Monterey, CA, USA
ORCID 0000-0001-8989-0617

Juan Manuel Nuñez-Alfonso
Instituto de Astronomía - UNAM
Ensenada, BC, Mexico
ORCID 0000-0003-4097-0063

***Abstract*—The design and experimental validation of bounded and partially bounded nonlinear controllers addressing tracking position tasks in DC motors are presented. Boundary properties in the development of controllers are required features to meet practical assumptions in the implementation stage. The general structure of the proposed controllers is derived by applying Sector Nonlinear control, and they stand out by their simplicity and global stability properties. A set of particular bounded and partially bounded nonlinear controllers exemplifies the proposed framework. A low-cost, real-time embedded control system attached to a DC motor is used to experimentally evaluate the performance of the designed nonlinear controllers where parameter uncertainty and nonlinear phenomena are present.**

***Index Terms*—Bounded nonlinear controllers, Partially bounded nonlinear controllers, DC Motors, Trajectory tracking control, Experiments.**

I. Introduction

The development of controllers applied to Direct Current (DC) Motors is of great importance due to their wide range of applications as actuators within engineering disciplines, such as robotics, control systems, and electrical drives, to mention a few. The analysis of their properties, and the analysis of control tasks for complex robotic systems, have been addressed thoroughly (see [1]–[8]). The model of a DC motor, neglecting the armature inductance, is given by a linear second-order dynamical system [9]–[11]. The approaches to constructing controllers for linear systems are numerous, many of them, also of a linear nature. However, in practice, most of the systems are nonlinear, thus, relaxing assumptions about the properties of the nonlinearities and uncertainties of the system, as well as an assumed local stability, are standard practices for constructing linear controllers [12]. Regardless of the simplicity of the dynamics used to model DC motors, several nonlinear phenomena are commonly found in them, such as friction, hysteresis, and stiffness, to mention a few [13]–[15]. Another important aspect of the design of controllers for physical systems is related to their operation capabilities, such as input constraints. Thus, bounded control signals are required to meet the maximum allowed values of the system. For linear systems with constrained inputs, the design of robust controllers using LMI tools is a frequent optimization approach, where assumptions about the solvability of the problem must be considered [16]. However, even after adequate tuning of the controller, peak values in the control signal can be present due to parametric uncertainties, disturbances, load variations, unmodeled dynamics, etc. Another common strategy for bounding controllers is introducing a saturation function that trims the control signal to maintain its magnitude between admissible ranges [17]–[20]. Techniques such as backstepping, composite nonlinear feedback control, sliding modes, barrier functions, and uncertainty compensation have also been applied for the control of actuators with saturated inputs, [21]–[27]. An additional challenge arises from introducing integral actions in the controllers, which can originate wind-up when the signals are saturated. This is a frequent issue with this class of controllers, such as in PI (Proportional-Integral) and PID (Proportional-Integral-Derivative) [28], hence, in these cases, anti-windup compensators are commonly introduced [29], [30]. The aim is to inhibit the growth of the integral term by resetting it so that the control signal is constrained between the predefined limits of the saturation function.

The design of nonlinear controllers with bounded and partially bounded properties addressing the tracking control task in DC motors is presented in this work. Experimental validation demonstrates their capabilities when applied to a DC motor, modeled as a linear system, but presenting common nonlinear phenomena for these systems. In contrast with the traditional saturated control approach, the presented design does not consider using a saturating function that limits an otherwise unrestricted control signal to keep it between the prescribed bounds. In addition, it does not require formulating and solving an optimization problem as in the LMI approach. The proposed design considers the application of BSN (Bounded Sector Nonlinear) control, where the explicit use of sector nonlinear functions allows the construction of inherently bounded nonlinear controllers where the simplicity of structure and global stability can be achieved [31]. The following considerations are introduced for the experimental setup: a) a particular set of nonlinear controllers are derived from the proposed design, b) inverse dynamics are considered, where a simple model identification is implemented, and c) nonlinear phenomena that challenge the robustness of the proposed controllers appear naturally in the DC motor used for testing. The performance of the experimental results is evaluated through integral indexes, the maximum values of the control signal, and the maximum error during the steady-state response.

This document is outlined as follows. The problem statement for the tracking control task and the controller's properties are declared in Section II. The general properties and the synthesis of the proposed family of nonlinear controllers to address the stated problem are presented in Section III. In Section IV, the experimental setting and the obtained results are analyzed. Finally, conclusions and future work are discussed in Section V.

II. Problem statement

A DC motor, neglecting the armature inductance, is modeled by a second-order dynamic system, given by [9]–[11]

$$J\,\ddot{q} + \left[f_v + \frac{K_a\,K_b}{R_a}\right]\dot{q} = \frac{K_a}{R_a}\,v, \tag{1}$$

where $\dot{q}$ and $\ddot{q}$ are the angular velocity and acceleration variables, respectively; the solution of (1), denoted by q, corresponds to the angular position of the shaft; v is the control input, defined as the applied voltage; J is the rotor inertia; f_v is the coefficient of viscous friction; and, K_a,K_b, R_a are electrical characteristics of the motor. All the parameters are strictly positive constants.

Let a $\mathcal{C}^2$ trajectory, $q_d(t) \in \mathbb{R}$, represent a desired trajectory, such that $q_d(t)$, $\dot{q}_d(t)$, $\ddot{q}_d(t) \in \mathcal{L}_\infty$. Then, the objective of this work is the construction and experimental validation of nonlinear bounded and partially bounded controllers to solve the tracking task defined by $\lim_{t\to\infty}|q_d(t) - q| = 0$.

III. Synthesis of the nonlinear controllers

The constructed family of bounded nonlinear controllers considers the applications of SN control where an explicit summation of bounded sector nonlinear functions is applied.

A. Preliminaries

Let us consider the following results, taken from [31], to build our particular set of nonlinear controllers.

Definition 1 (Bounded Sector Nonlinear (BSN) Function, [31])**.** *Consider a function $\psi : \mathbb{R} \to \mathbb{R}$, and constants l, m, $\gamma \in \mathbb{R} > 0$. For all $z \in \mathbb{R}$, function ψ belongs to sector $[l,\, m]$ if $p = \psi(z)$ is contained between lz and mz. Note that the above implies that $z\psi(z) \geq 0$. In addition, ψ is a function bounded by a value γ if $|\psi(z)| \leq \gamma$, for all $z \in \mathbb{R}$.*

Lemma 1 ([31])**.** *Let $g(z) \in \mathcal{C}^1$ be a bounded nonlinear function, belonging to sector $[0, \alpha]$ and constrained by a constant value $\gamma \in \mathbb{R}$, such that it is strictly increasing under the condition $|g(z)| \leq \gamma$. Then, it is possible to build a positive definite function $G(z) > 0$ based on the integral of $g(z)$.*

Theorem 2 ([31])**.** *Let $g^E(m_1\,z)$, $g^D(m_3\,\dot{z})$ be BSN functions with m_1, m_3 as positive constants. Then, the linear second-order dynamical system $\ddot{z} + g^E(m_1\,z) + g^D(m_3\,\dot{z}) = 0$ is globally asymptotically stable.*

Theorem 3 ([31])**.** *Let $g^E(m_1\,z)$, $g^I(m_2\,z)$, $g^D(m_3\,\dot{z})$ be BSN functions with m_1, m_2, m_3 as positive constants, and $g^I(m_2\,z) : G^I(m_2\,z) > 0$ holds where $G^I(m_2\,z)$ is the time integral of $g^I(m_2\,z)$. Then, the linear second-order dynamical system $\ddot{z} + g^E(m_1\,z) + \int_0^t g^I(m_2\,z)d\tau + g^D(m_3\,\dot{z}) = 0$ is globally asymptotically stable.*

The proof of Theorems 2 and 3 yields on the Lyapunov function $V(z, \dot{z}) = G^E(m_1\,z) + \frac{1}{2}\dot{z}^2$, where $G^E(m_1\,z)$ is a positive definite function constructed by means of Lemma 1, and the application of LaSalle's invariance principle.

B. Tracking task in DC motors

To address the control tracking task in the DC motor, let us consider the angular errors of the motor relating to the desired trajectory, that is, $\tilde{q}(t) = q_d(t) - q$, $\dot{\tilde{q}}(t) = \dot{q}_d(t) - \dot{q}$, $\ddot{\tilde{q}}(t) = \ddot{q}_d(t) - \ddot{q}$. The construction of the bounded controllers considers a general control structure with dynamic feedback which takes the system (1) into a globally asymptotically stable form, this is

$$\begin{aligned} v &= v_b = u_{inv} + g^E(m_1\,\tilde{q}) + g^D(m_3\,\dot{\tilde{q}}), & (2)\\ u_{inv} &= \frac{J\,R_a}{K_a}\ddot{q}_d - \frac{R_a}{K_a}\left[f_v + \frac{K_a\,K_b}{R_a}\right]\left(\dot{q}_d - \dot{\tilde{q}}\right), & (3) \end{aligned}$$

where $g^E(m_1\,\tilde{q})$ and $g^D(m_3\,\dot{\tilde{q}})$ are BSN functions w.r.t. the errors in angular position and velocity, respectively, satisfying Definition 1.

Theorem 4. *Let the system* (1)*, with control input* (2), (3)*, where $g^E(m_1\,\tilde{q})$, $g^D(m_3\,\dot{\tilde{q}})$ with m_1, $m_3 > 0$, belong to the particular class of bounded nonlinear sector functions satisfying Definition 1. Then, the closed-loop dynamics is globally, asymptotically stable.*

Proof. The closed-loop dynamics, obtained by substituting (2) into the dynamics of the motor (1), are given as

$$\ddot{\tilde{q}} + \frac{K_a}{J\,R_a}\,g^E(m_1\,\tilde{q}) + \frac{K_a}{J\,R_a}\,g^D(m_3\,\dot{\tilde{q}}) = 0. \tag{4}$$

Then, proposing a modified Lyapunov candidate function as

$$V(\tilde{q}, \dot{\tilde{q}}) = G^E(m_1\tilde{q}) + \frac{2\,J\,R_a\,m_1}{K_a}\,\dot{\tilde{q}}^2, \tag{5}$$

yields $\dot{V}(\tilde{q}, \dot{\tilde{q}}) = -m_1\,\dot{\tilde{q}}\,g^D(m_3\,\dot{\tilde{q}}) < 0$. Hence, since $m_1 > 0$ by design, and due to the properties of the BSN function, global asymptotic stability is concluded. □

The construction of partially bounded nonlinear controllers stems from the introduction of an integral action; this is,

$$v_p = v_b + \int_0^t g^I(m_2\,\tilde{q}(\tau))\,d\tau, \tag{6}$$

where v_b is the bounded controller given in (2), while $g^I(m_2\,\tilde{q})$ is a function that satisfies Definition 1, as well.

Theorem 5. *Consider the system* (1) *with the control input augmented with integral action* (6)*, where functions* $g^E(m_1\,\tilde{q})$*,* $g^I(m_2\,\tilde{q})$*,* $g^D(m_3\,\dot{\tilde{q}})$ *with* m_1*,* m_2*,* $m_3 > 0$*, belong to the particular class of sector nonlinear functions satisfying Definition 1. Then, the closed-loop system is globally, asymptotically stable.*

Proof. Applying the same candidate Lyapunov function as in Theorem 4 (i.e. (5)) to the closed-loop dynamics

$$\begin{aligned}\ddot{\tilde{q}} &+ \frac{K_a}{J\,R_a}\,g^E(m_1\,\tilde{q}) + \frac{K_a}{J\,R_a}\int_0^t g^I(m_2\,\tilde{q}(\tau))\,d\tau \\ &+ \frac{K_a}{J\,R_a}\,g^D(m_3\,\dot{\tilde{q}}) = 0,\end{aligned}$$

yields

$$\begin{aligned}\dot{V}(\tilde{q},\dot{\tilde{q}}) &= -m_1\left(\dot{\tilde{q}}\,g^D(m_3\,\dot{\tilde{q}}) + \dot{\tilde{q}}\int_0^t g^I(m_2\,\tilde{q}(\tau))\,d\tau\right) \\ &= -m_1\left(\dot{\tilde{q}}\,g^D(m_3\,\dot{\tilde{q}}) + G^I(m_1\,\tilde{q}(t))\right) < 0 \\ &s.t.\quad g^I(m_2\,\tilde{q}) : G^I(m_2\,\tilde{q}(t)) > 0.\end{aligned}$$

Therefore, $\dot{V}(\tilde{q},\dot{\tilde{q}}) < 0$, thus concluding global asymptotic stability. □

By Definition 1, the functions $g^E(m_1\,\tilde{q})$, $g^D(m_3\,\dot{\tilde{q}})$, and the function $g^I(m_2\,\tilde{q})$ under the integral in (6), are bounded. The compensation term u_{inv} is bounded since it is obtained from the feedback linearization of a physical system with operation restrictions and given the established properties of the desired trajectory.

The experimental validation of the nonlinear controllers built for the tracking task is applied to a DC motor in the form of a set of nonlinear controllers following the general structures given by (2)-(3) and (6).

IV. Experimental evaluation

The experimental platform is shown in Figure 1 consisting of a low-cost Uxcell 301 DC Gearmotor and a two-channel Hall effect encoder with an 823.1 ppr resolution. It is controlled in real-time through an embedded control board system driven by an Arduino® Mega2560 board. Custom functions for real-time execution have been implemented, instead of the predefined ones offered by the Arduino® IDE. The only external library used is for data logging into a MicroSD card. The real-time embedded control system is configured with a sample time of $t_s = 0.04096$ seconds.

The DC motor's parameters are unknown and Matlab®'s System Identification toolbox was used to estimate them. To this end, a parameterized second-order dynamical system is given as

$$a\,\ddot{x} + b\,\dot{x} + c\,x = d\,u. \tag{7}$$

has been used to fit real measurements. Here, a, b, c, and d are positive constant values construed from the motor parameters. The aim is to estimate the values of $a \approx J$, $b \approx f_v + \frac{K_a\,K_b}{R_a}$, $c \approx 0$, and $d \approx \frac{K_a}{R_a}$, for the computation of a dynamic feedback, u_{inv}, as in (3).

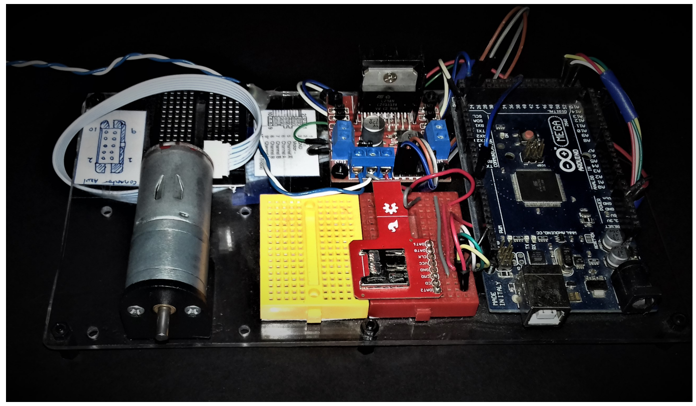

Fig. 1: DC motor testbed with a real-time embedded control system.

Sinusoidal signals of 5 Volts of amplitude, at frequencies of $f = \frac{\pi}{k}$ Hz, $k = 2, 4, .., 16, 18$ have been applied during 100 seconds to obtain input-output measurements from the DC motor. The best identification results produced a model with a precision of 91.41%, according to Matlab®, concerning the input-output measured data. The fitted model is given in the form (7), with $a = 1$, $b = 4.509$, $c = 6.087\times10^{-11}$ and $d = 9.527$. In addition, a ramp voltage signal has been applied to observe nonlinear phenomena in the DC motor. In Figure 2, we have 2a) and 2b) as examples of the obtained measurements from the DC motor and the simulated dynamics from the identified model (7); 2c) is a test applying a voltage ramp signal; and 2d) is a phase portrait of angular position versus angular velocity. As observed, the DC motor suffers from severe nonlinear dynamics at low velocities; it appears to 'stick' until a voltage threshold is crossed and then starts moving abruptly. Identification and compensation of such nonlinearities is an open issue in control systems and is out of the scope of this work. However, the interested reader can refer to [32] and [33] for details on compensation. The discrepancy between the measurements and the estimated model can be explained by the unmodeled dynamics, the parametric uncertainty, and the nonlinear phenomena that appear naturally in DC motors. The robustness of the proposed family of controllers will be tested under these characteristics.

For all the controllers under study, the desired reference signal is defined as $q_d(t) = 10\,\cos\left(\frac{\pi}{15}\,t\right)$ radians. For simplicity, consider the same selected BSN function is applied for each nonlinear controller in their corresponding terms. However, it is possible to choose and combine any BSN function as long as (a) it fulfills Definition 1, and (b) the required condition for the integral actions, as established in the stability analysis, is held. The performance analysis is done through the numerical computation of the discrete versions of MSE (Mean Square Error), IAE (Integral Absolute Error), ITAE (Integral of the Time Weighted Absolute), and ISTC (Integral of Square Time Derivative of the Control Input Error) [34]. In addition, the maximum voltage applied during the experiment, and the maximum angular position error, $\tilde{q}(t)$, during the steady-state response, are calculated as well.

A. *The bounded nonlinear controllers*

For this setting, two bounded controllers are evaluated. These are denoted as v_1 and v_2, and defined according to the structure in (2), where the selected BSN functions are based on quotients of a squared root, and exponential functions, respectively. The proposed controllers are given as

$$v_1 = \hat{u}_{inv} + \gamma^E \frac{m_{11}\,\tilde{q}}{\sqrt{m_{11}^2\,\tilde{q}^2+1}} + \gamma^D \frac{m_{12}\,\dot{\tilde{q}}}{\sqrt{m_{12}^2\,\dot{\tilde{q}}^2+1}} \qquad (8)$$

$$v_2 = \hat{u}_{inv} + \gamma^E \frac{e^{m_{21}\,\tilde{q}}-1}{e^{m_{21}\,\tilde{q}}+1} + \gamma^D \frac{e^{m_{22}\,\dot{\tilde{q}}}-1}{e^{m_{22}\,\dot{\tilde{q}}}+1} \qquad (9)$$

$$\hat{u}_{inv} = 0.105\,\ddot{q}_d + 0.4732\,\dot{q} + 6.3892\times 10^{-12}\,q \qquad (10)$$

where $\hat{u}_{inv}$ is the computed feedback dynamics derived from the model (7) with estimated parameters $a = 1$, $b = 4.509$, $c = 6.087\times 10^{-11}$ and $d = 9.527$; γ^E and γ^D are positive constants that define the bound values of each BNS function. The selected bounds are $\gamma^E = 5\,V$ and $\gamma^D = 2\,V$, thus bringing the BSN to belong to sectors $[0,\ 8.4]$ and $[0,\ 1.575]$, respectively. For each BSN function, the gain values m_{ij}, $i,\ j = 1,\ 2$, are set to m_{11}=1.8867 and m_{12}=0.63, for the case of the controller v_1, and to m_{21}=3.7333, and m_{22}= 1.26, for the controller v_2. These values are used to adjust the slope of the BSN functions. The responses obtained from the DC motor are shown in Figure 3. The performance analysis is presented in Table I.

B. *The partially bounded nonlinear controllers*

Due to the condition $g^I(m_2\,\tilde{q}) : G^I(m_2\,\tilde{q}(t)) > 0$, established by the stability proof of Theorem 5, the BSN function for the integral action must be carefully chosen. The other two BSN functions in the controller can be any BSN, as long as they fulfill Definition 1. The two partially bounded controllers under experimental evaluation, denoted as v_3 and v_4, are defined as

$$v_3 = \hat{u}_{inv} + \gamma^E \tanh(m_{31}\,\tilde{q}) + \gamma^I \int_0^t \tanh(m_{32}\,\tilde{q}(\tau))d\tau + \gamma^D \tanh(m_{33}\,\dot{\tilde{q}}) \qquad (11)$$

$$v_4 = \hat{u}_{inv} + \frac{2\,\gamma^E}{\pi}\arctan(m_{41}\,\tilde{q}) + \frac{2\,\gamma^I}{\pi}\int_0^t \arctan(m_{42}\,\tilde{q}(\tau))d\tau + \frac{2\,\gamma^D}{\pi}\arctan(m_{43}\,\dot{\tilde{q}}) \qquad (12)$$

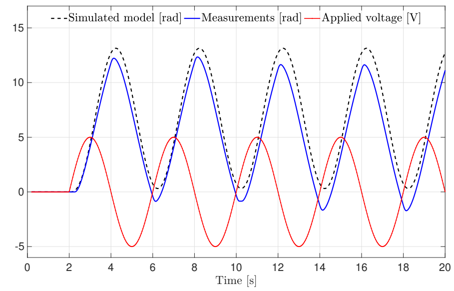

(a)

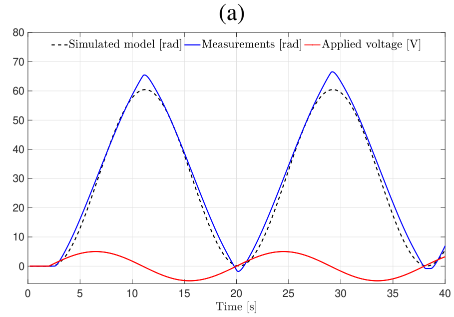

(b)

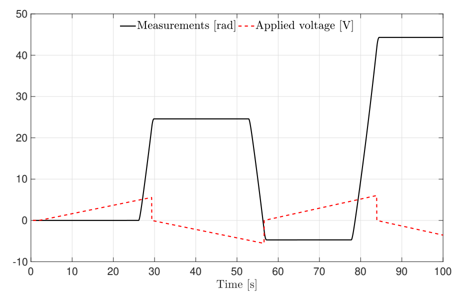

(c)

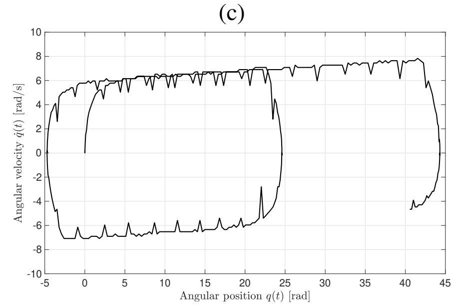

(d)

Fig. 2: Open loop input-output data. The system identification process is shown for $V = 5\sin(\frac{\pi}{2}t)$, 2a), for $V = 5\sin(\frac{\pi}{9}t)$, 2b). The nonlinearity is observed when applying a ramp voltage signal, 2c) and 2d).

where the estimated dynamic feedback $\hat{u}_{inv}$ is the same as for the bounded case given in (10). The parameters γ^E, γ^I, and γ^D are positive constants that define the bound values of each BSN function in the controller. The selected values for these are given as $\gamma^E = 4.5\,V$, $\gamma^I = 0.5\,V$, and $\gamma^D = 2\,V$. Then, under these conditions, the BSN functions belong to sectors $[0,\ 8.4]$, $[0,\ 0.0315]$, and $[0,\ 1.575]$, respectively.

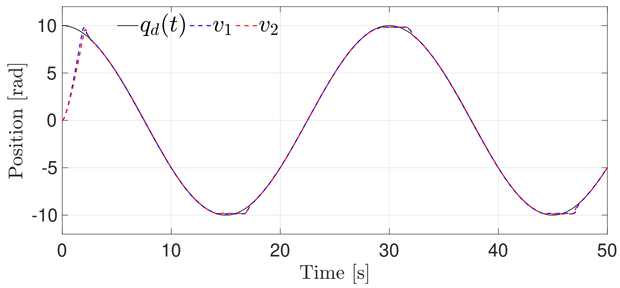

(a)

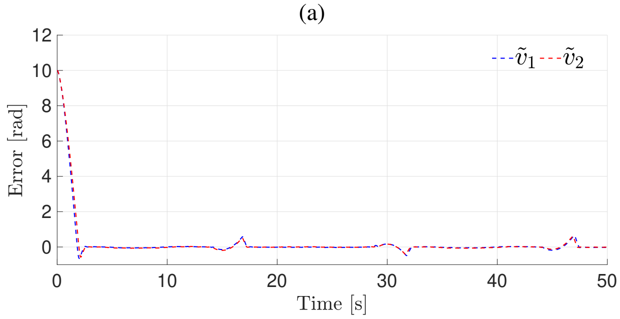

(b)

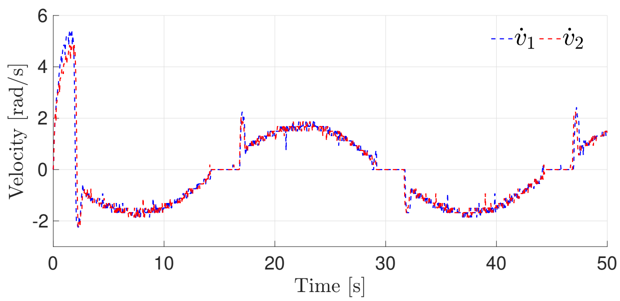

(c)

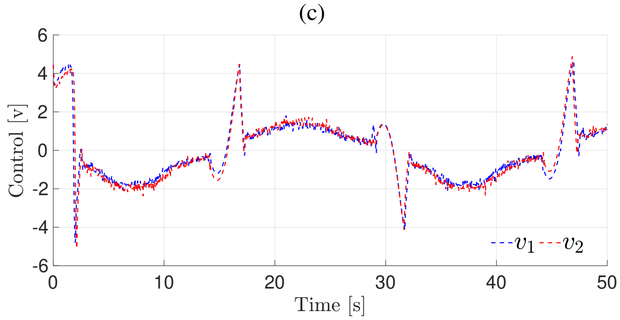

(d)

Fig. 3: Experimental results applying the Bounded Nonlinear Controllers v_1 and v_2 given in (8) and (9), with dynamic feedback (10).

The gain values for the slopes of the BSN functions are set to m_{31}=1.8667, m_{32}= 0.06, m_{33}=0.7875, m_{41}=2.9322, m_{42}=0.0942, and m_{43}=1.237. Figure 4 shows the experimental results, while the performance comparison is summarized in Table I.

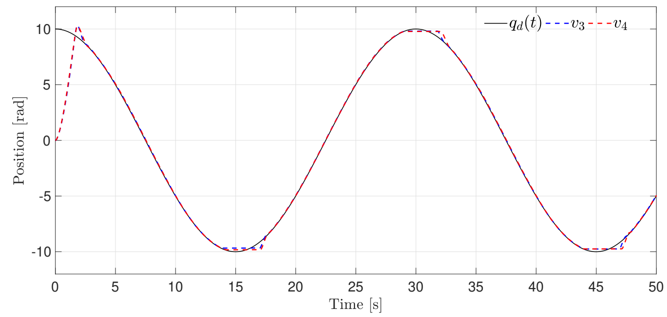

(a)

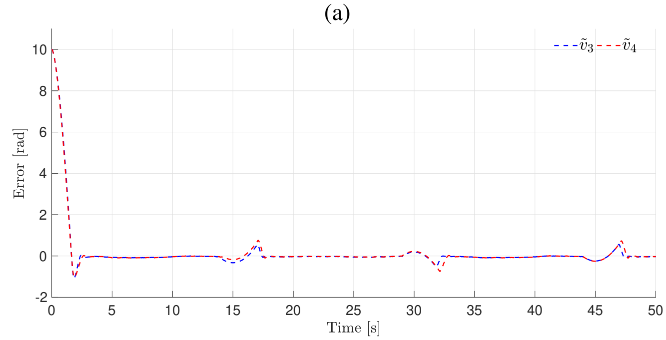

(b)

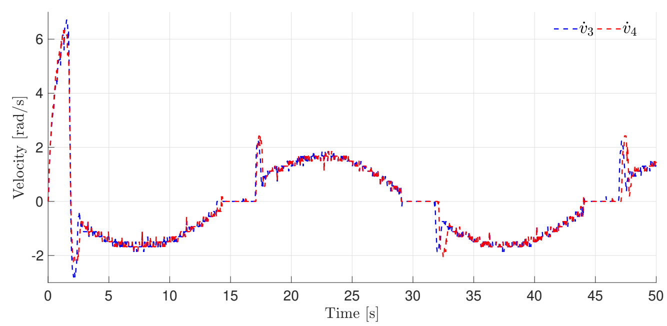

(c)

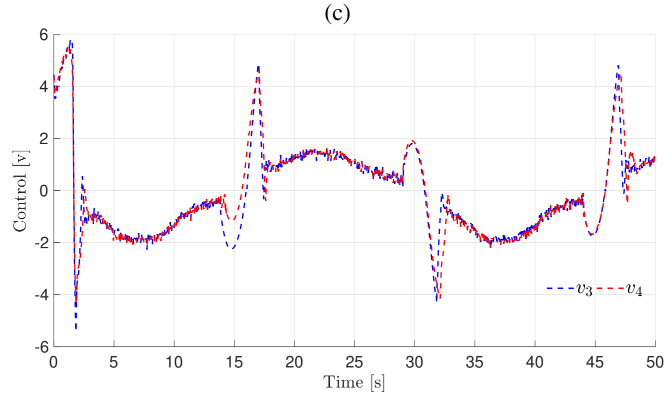

(d)

Fig. 4: Experimental results applying the partially Bounded Nonlinear Controllers v_3 and v_4 given in (11) and (12), with dynamic feedback (10).

C. Discussion

The experimental results demonstrate that all the proposed nonlinear controllers solved the specified tracking task. Fur-

TABLE I: Performance of the BSN controllers v_1 and v_{v_2} given in (8) and (9), and of the partially BSN controllers v_3, v_4 in (11) and (12), all with an estimated dynamic feedback (10) computed according to the identified model (7).

Performance index	Bounded nonlinear controllers		Partially bounded nonlinear controllers	
	v_1	v_2	v_3	v_4
MSE	1.4200	1.5086	1.4659	1.4037
IAE	0.2382	0.2476	0.2411	0.2477
ITAE	2.2851×10^3	2.0019×10^3	2.0183×10^3	2.6267×10^3
ISTC$\vert_{t\in[10,60]}$	935.2120	976.7442	1052.3541	781.5058
max(|voltage|)	4.789	5.108	5.299	4.766
$\max(\vert\tilde{q}(t)\vert)\vert_{t\in[10,60]}$	0.657	0.617	0.530	0.964

thermore, they deal with model uncertainty and severe nonlinear phenomena affecting the DC motor. Their most important feature is their boundedness property which can be selected at will by choosing a constant bound value for the BSN functions that explicitly appear in the structure of the controller. The maximum voltage applied by each evaluated controller is shown in Table I (see rows max(|voltage|)). Regardless of the initial error, none of the four evaluated controllers reaches the bound established by the summation of the bounds of each BSN function (i.e. 7 volts). All the controllers have been tuned to provide similar slope values and bounds, thus, similar performance is observed (see Table I). The difference between their responses is due to the particularities of the selected nonlinear functions. Notice from the figures 3 and 4 that the position errors generated by each controller remain small; to confirm this, the MSE index, which highly penalizes position errors with large values, is employed (see Table I). The IAE index shows the average of the absolute error concerning the whole experiment is small. The ITAE index strongly penalizes large errors occurring after, such as the one induced by the nonlinearity; hence, its high value. The ISTC index has been applied to the voltage variable in steady-state response; it measures the oscillations in the control signal. Normally, the value of this index reflects the oscillatory voltage required to follow an oscillatory trajectory but, in our case, it mostly reflects the effects of the nonlinearity (see the control signal in Figures 3 and 4). The smoothest response is obtained with the arctangent function in the partially bounded controller (12). From all the selected BSN functions, the slowest rate of convergence to the bound value corresponds to the arctangent function.

The performance analysis shows a voltage peak in the low-velocity range, where the nonlinearity appears. The experiments suggest that this nonlinearity could result from the combination of deadzone, backlash and/or hysteresis in the DC motor. The compensation of these combined phenomena is an open problem in control systems. This is perceived in the experiments as a lack of motion in the motor's angular position $q(t)$ when voltages are applied. In the graphs of position (that is, in Figures 3a) and 4a), the nonlinear phenomenon is evidenced by the flat section in the crests and valleys of the trajectory. The maximum error in angular position $\tilde{q}(t)$, in the presence of the nonlinearity, is presented in Table I (see rows $\max(|\tilde{q}(t)|)|_{t\in[10,60]}$); the evaluated period of 10 to 60 seconds was selected since the DC motor is in steady state (that is, it has already reached the desired motion). When the nonlinearity is present, the lack of motion in the shaft increases the position error. Thus, the controller increases the voltage to recover the desired trajectory; the control signal will continue increasing until the voltage is enough to restart the motion. This is a similar effect to that of integrator windup occurring in saturated systems, and it is a major issue in control, since as the error increases, the integral action rises (it 'winds up'), successively causing the control action to increase as well. In our proposal, using an integral action of a bounded signal concerning the position error sets the growth rate up to a maximum constant value, regardless of an uncontrolled or sudden increase in the position error. This helps to avoid the wind-up problem and reduces overshoots in the response of the DC motor, as observed in the experimental results shown in Figures 3 and 4.

For the particular set of nonlinear controllers under study, their stability can be analyzed through the construction of a Lyapunov function (5), where a positive definite function needs to be constructed for each particular BSN function, as established in Lemma 1. Notice that this positive definite function, $G^E(m_1\,\tilde{q})$, is based on the time integral of the corresponding BSN function. The positive definite functions corresponding to each BSN are shown in Table II; these were found through symbolic software. The sector of each BSN function defines the section of the Cartesian plane where the function resides, as established in Definition 1. The sector to which they belong was algebraically computed as $\left[0,\,\gamma^E\,m_1\right]$, $\left[0,\,\frac{\gamma^E\,m_1}{2}\right]$, $\left[0,\,\gamma^E\,m_1\right]$, and $\left[0,\,\frac{2\,\gamma^E\,m_1}{\pi}\right]$, for v_i, $i=1,...,4$, respectively.

V. Conclusions and Future Work

The outline for the design of bounded and partially bounded nonlinear controllers is studied through an experimental evaluation in a DC motor affected by nonlinear phenomena. Sector nonlinear control is applied to build a general structure addressing the tracking task in DC motors, modeled by a

TABLE II: BSN functions used in the experimentally evaluated nonlinear controllers, and their corresponding construed positive definite functions required by Lyapunov function (5) for the closed-loop stability proof of each controller.

Controller	BSN function $g^E(m_1\,\tilde{q})$	Definite positive function $G^E(m_1\,\tilde{q})$
v_1	$\gamma^E\,\frac{m_1\,\tilde{q}}{\sqrt{m_1^2\,\tilde{q}^2+1}}$	$\frac{\gamma^E}{m_1}\sqrt{m_1^2\,\tilde{q}^2(t)+1}-\frac{\gamma^E}{m_1}$
v_2	$\gamma^E\,\frac{e^{m_1\,\tilde{q}}-1}{e^{m_1\,\tilde{q}}+1}$	$\gamma^E\left(\frac{2\ln(e^{m_1\,\tilde{q}(t)}+1)}{m_1}-\tilde{q}\right)$ $-\frac{2\,\gamma^E}{m_1}\ln(2)$
v_3	$\gamma^E\tanh(m_1\,\tilde{q})$	$\frac{\gamma^E}{m_1}\ln(\cosh(m_1\,\tilde{q}(t)))$
v_4	$\frac{2\,\gamma^E}{\pi}\arctan(m_1\,\tilde{q})$	$\frac{2\gamma^E}{\pi}\,\tilde{q}(t)\arctan(m_1\,\tilde{q}(t))$ $-\frac{\gamma^E}{m_1\,\pi}\left(\ln(m_1^2\,\tilde{q}^2(t)+1)\right)$

second-order linear dynamical system. BSN functions satisfying a particular definition are selected as an example set of controllers, and to validate their performance by implementing them in a DC motor testbed with real-time execution. A simple model identification, performed with numerical software that matches input-output measurements, is applied to estimate feedback dynamics that partially compensate for the dynamics of the DC motor. The effectiveness of the controllers under study is evidenced by their exhibited robustness under the uncertainty in the estimated model and unidentified complex nonlinear phenomena. The design of a tuning method, using observers, and implementing model identification techniques with better accuracy are proposed as future work.

ACKNOWLEDGEMENTS

L. Monay-Arredondo thanks CONAHCYT and TecNM/I.T. Tijuana for the support given under scholarship No. 406498. C. Loreto-Medina and M. Meza-Sánchez thank Club de Robótica y Proyectos Institucionales de Innovación del TecNM - Instituto Tecnológico de Tijuana.

REFERENCES

[1] Z. Wang, C.-Y. Su, and S. S. Ge, "Adaptive control of mobile robots including actuator dynamics," in *Autonomous Mobile Robots: Sensing, Control, Decision Making and Applications*, S. S. Ge and F. L. Lewis, Eds. Boca Raton: CRC Press, 2006, ch. 7, pp. 267–293.

[2] J. Viola, L. Angel, and J. M. Sebastian, "Design and robust performance evaluation of a fractional order pid controller applied to a dc motor," *IEEE/CAA Journal of Automatica Sinica*, vol. 4, no. 2, pp. 304–314, 2017.

[3] A. Bisoi, A. Samantaray, and R. Bhattacharyya, "Control strategies for dc motors driving rotor dynamic systems through resonance," *Journal of Sound and Vibration*, vol. 411, pp. 304–327, 2017.

[4] A. Izadbakhsh and P. Kheirkhahan, "On the voltage-based control of robot manipulators revisited," *Int. J. Control Autom. Syst.*, vol. 16, pp. 1887–1894, 2018.

[5] H. Liu, Q. Huang, and Z. Tong, "Simulation and analysis of a full-active electro-hydrostatic powered ankle prosthesis," in *2019 19th International Conference on Advanced Robotics (ICAR)*, 2019, pp. 81–86.

[6] L. Herrera, Y. Orlov, O. Montano, and A. Shiriaev, "Model orbit output feedback tracking of underactuated mechanical systems with actuator dynamics," *International Journal of Control*, vol. 93, no. 2, pp. 293–306, 2020.

[7] F. Beltran-Carbajal, R. Tapia-Olvera, A. Valderrabano-Gonzalez, H. Yanez-Badillo, J. Rosas-Caro, and J. Mayo-Maldonado, "Closed-loop online harmonic vibration estimation in dc electric motor systems," *Applied Mathematical Modelling*, vol. 94, pp. 460–481, 2021.

[8] S.-K. Kim, J. K. Park, and C. K. Ahn, "Learning and adaptation-based position-tracking controller for rover vehicle applications considering actuator dynamics," *IEEE Transactions on Industrial Electronics*, vol. 69, no. 3, pp. 2976–2985, 2022.

[9] M. W. Spong and M. Vidyasagar, *Robot Dynamics and Control*, 1st ed. New York, NY, USA: Wiley, 1989.

[10] D. M. Dawson, J. J. Hu, and T. C. Burg, *Nonlinear Control of Electric Machinery*, 1st ed. New York, NY, USA: Marcel Dekker, Inc., 1998.

[11] R. Dorf and R. Bishop, *Modern Control Systems*, 9th ed. Upper Saddle River, NJ, USA: Prentice-Hall, Inc., 2000.

[12] S. Bhattacharyya, A. Datta, and L. Keel, *Linear Control Theory: Structure, Robustness, and Optimization, Automation and Control Engineering Series*, 1st ed. Boca Raton, Florida, USA: CRC Press, 2009.

[13] A. K. Padthe, B. Drincic, J. Oh, D. D. Rizos, S. D. Fassois, and D. S. Bernstein, "Duhem modeling of friction-induced hysteresis," *IEEE Control Systems Magazine*, vol. 28, no. 5, pp. 90–107, 2008.

[14] J. Y. Yoon and D. L. Trumper, "Friction modeling, identification, and compensation based on friction hysteresis and dahl resonance," *Mechatronics*, vol. 24, no. 6, pp. 734–741, 2014.

[15] X. Zheng, X. Yu, J. Jiang, and X. Yang, "Practical finite-time command filtered backstepping with its application to dc motor control systems," *IEEE Transactions on Industrial Electronics*, vol. 71, no. 3, pp. 2955–2964, 2024.

[16] S. Boyd, L. El Ghaoui, E. Feron, and V. Balakrishnan, *Linear Matrix Inequalities in System and Control Theory, Studies in Applied Mathematics Series*, 1st ed. Philadelphia, PA: SIAM, 1994.

[17] D. S. Bernstein and A. N. Michel, "A chronological bibliography on saturating actuators," *International Journal of Robust and Nonlinear Control*, vol. 5, no. 5, pp. 375–380, 1995.

[18] T. Hu and Z. Lin, *Control Systems with Actuator Saturation*, 1st ed. Boston: Birkhäuser, 2001.

[19] Y. Li and Z. Lin, *Stability and Performance of Control Systems with Actuator Saturation*, 1st ed. New York, NY, USA: Birkhäuser Basel, 2018.

[20] M. Ebrahimi and M. Homaeinezhad, "Compensation of friction and stick-slip uncertainties in trajectory tracking control of servo dc machines considering actuation constraints," *Proceedings of the Institution of Mechanical Engineers, Part I: Journal of Systems and Control Engineering*, vol. 238, no. 3, pp. 479–503, 2024.

[21] B. Chen, T. Lee, K. Peng, and V. Venkataramanan, "Composite nonlinear feedback control for linear systems with input saturation: theory and an application," *IEEE Transactions on Automatic Control*, vol. 48, no. 3, pp. 427–439, 2003.

[22] R. Wang and J. Liu, "Trajectory tracking control of a 6-dof quadrotor uav with input saturation via backstepping," *Journal of the Franklin Institute*, vol. 355, no. 7, pp. 3288–3309, 2018.

[23] S. P. Sadala and B. M. Patre, "A new continuous sliding mode control approach with actuator saturation for control of 2-dof helicopter system," *ISA transactions*, vol. 74, pp. 165–174, 2018.

[24] M. Salah, A. Al-Jarrah, E. Tatlicioglu, and S. Banihani, "Backstepping control for a four-bar linkage mechanism driven by a dc motor," *Intell Robot Syst*, vol. 94, p. 327–338, 2019.

[25] X. Zhu and D. Li, "Robust fault estimation for a 3-dof helicopter considering actuator saturation," *Mechanical Systems and Signal Processing*, vol. 155, p. 107624, 2021.

[26] K. Shao, J. Zheng, R. Tang, X. Li, Z. Man, and B. Liang, "Barrier function based adaptive sliding mode control for uncertain systems with input saturation," *IEEE/ASME Transactions on Mechatronics*, vol. 27, no. 6, pp. 4258–4268, 2022.

[27] L. Tang, R. Sun, and S. Zhang, "Boundary vibration constraint control design of motor-driven industrial moving belt systems subject to actuator input saturation," *IEEE Transactions on Consumer Electronics*, pp. 1–1, 2022.

[28] K. J. Aström and L. Rundqwist, "Integrator windup and how to avoid it," in *1989 Amer Contr Conf*, 1989, pp. 1693–1698.

[29] S. Tarbouriech and M. Turner, "Anti-windup design: an overview of some recent advances and open problems," *IET Control Theory & Applications*, vol. 3, pp. 1–19(18), January 2009.

[30] M. Hussain, M. Rehan, C. Ki Ahn, and M. Tufail, "Robust antiwindup for one-sided lipschitz systems subject to input saturation and applica-

tions," *IEEE Transactions on Industrial Electronics*, vol. 65, no. 12, pp. 9706–9716, 2018.

[31] E. Clemente, M. Rodríguez-Liñán, M. Meza-Sánchez, L. Monay-Arredondo, and L. Herrera, "A class of bounded and partially bounded nonlinear controllers for first and second order dynamical systems," *IEEE Control Systems Letters*, vol. 6, pp. 1028–1033, 2022.

[32] G. Tao and P. V. Kokotovic, *Adaptive Control of Systems with Actuator and Sensor Nonlinearities*, 1st ed. USA: John Wiley & Sons, Inc., 1996.

[33] M. C. Rodríguez-Liñán and W. P. Heath, "Controller structure for plants with combined saturation and deadzone/backlash," in *2012 IEEE International Conference on Control Applications*, oct 2012, pp. 1394–1399.

[34] P. D. Domański, *Control Performance Assessment: Theoretical Analyses and Industrial Practice*, 1st ed. Cham, Switzerland: Springer nature, 2020.